Geomorphology 139–140 (2012) 506–517

Contents lists available at SciVerse ScienceDirect

Geomorphology

journal homepage: www.elsevier.com/locate/geomorph

Deepening of inner gorges through subglacial meltwater — An example from the UNESCO Entlebuch area, Switzerland

Mirjam Dürst Stucki [a,*], Fritz Schlunegger [a], Fabian Christener [a], Jan-Christoph Otto [b], Joachim Götz [b]

[a] Institute of Geological Sciences, University of Berne, Baltzerstrasse 3, CH-3012 Bern, Switzerland
[b] Department 'Geography and Geology', University of Salzburg, Hellbrunnerstrasse 34, A-5020 Salzburg, Austria

ARTICLE INFO

Article history:
Received 18 June 2011
Received in revised form 25 November 2011
Accepted 29 November 2011
Available online 7 December 2011

Keywords:
Subglacial meltwater erosion
Inner gorge
Deglaciation
Subalpine Molasse

ABSTRACT

This paper explores the mechanisms by which inner gorges in the Alps were formed. It focuses on the ca. 1.5-km-long, 80-m-deep, and a few hundred meter wide *Lammschlucht* located in the northern foothills of the central Alps. We reconstructed the glacial cover using lateral moraines and hanging talus cones that record the elevation of the ice surface at the deglaciation stage of the LGM (Last Glacial Maximum). We used the reconstructed ice thickness patterns to calculate the erosional potential of the subglacial meltwater. The applied model is based on the principle of energy conservation and yields the pattern of downstream changes of the dynamic pressure, which is considered a measure for erosion potential. The model results suggest a maximum of the dynamic pressure at the end of the inner gorge. We interpret, therefore, that the subglacial meltwater scoured the reach toward the end of the *Lammschlucht* because of the enhanced dynamic pressure, which was ultimately controlled by the ice overburden. Post-glacial fluvial erosion then resulted in a readjustment through a regressive shift of the erosional front along the inner gorge farther upstream. The current location of this front lies almost in the middle of the *Lammschlucht* inner gorge where a step-pool channel changes into a straight plane-bed channel flowing on a deeply scoured bedrock.

1. Introduction

Inner bedrock gorges have a distinct (valley-in-valley) cross section and may occur in rock and debris slope (Kelsey, 1988; Korup and Schlunegger, 2007; Ouimet et al., 2008; Montgomery and Korup, 2011). They form a convex break in hillslope gradient and are lined by hillslope toes steeper than those of upper valley flanks (Kelsey, 1988; Korup and Schlunegger, 2007). They have been recognized in many parts of the European Alps but preferentially occur at the orogen border such as in proximal Molasse deposits, Penninic Schists Lustrés, Flysch sandstone–mudstone alternations, and Helvetic limestones (Korup and Schlunegger, 2007). The formation of inner gorges requires special conditions, including continued base-level fall, predominance of debris slides, lack of sediment storage in the channel reach, and a topography that is characterized by an initially low relief (Kelsey, 1988).

The mechanisms leading to the formation of inner gorges and the timing of their origin are highly debated. Their genesis is probably related to multiple glacial–interglacial phases (Korup and Schlunegger, 2007). For instance, Montgomery and Korup (2011) suggested that inner gorges in the Swiss Alps progressively formed through multiple glacial stages and were thus robust to repeated glaciations. In particular, local evidence for remnant deposits of indurated and weathered glaciofluvial sediment or till within a number of Alpine gorges implies a pre-LGM (Last Glacial Maximum) origin (Cadisch, 1926; De Graaff, 1996; Montgomery and Korup, 2011). Based on erosion rate calculations, Montgomery and Korup (2011) also proposed that the incision of inner gorges in the Swiss Alps began probably before the LGM because the implied average erosion rates for an exclusively post-glacial gorge formation are inconsistent with long-term exhumation rates in the Alps. The origin of the inner gorges is likewise partially unresolved. Multiple mechanisms have been used to explain their genesis (Korup and Schlunegger, 2007), including relief rejuvenation by fluvial incision in response to rapid base-level drop (Ahnert, 1988; Kelsey, 1988; Densmore et al., 1997; Bonnet et al., 2001; Stock et al., 2005; Ouimet et al., 2008), repeated glaciations (Mitchell et al., 1999), landsliding focused at hillslope toes (Kelsey, 1988; Densmore and Hovius, 2000), and catastrophic outburst flows from natural dam failures (Knudsen and Marren, 2002; Rudoy, 2002). Despite clear evidence for fluvial downcutting and incision in many places (Valla et al., 2009), an origin related to glacial and subglacial fluvial erosion cannot be completely excluded as they may exhibit undulating longitudinal profiles and contain sections that slope upward. Sharpe and Shaw (1989) described linear hollows and depressions cut into bedrock near Quebec, Canada, that they related to subglacial fluvial erosion. Likewise, in the Molasse foreland basin on the northern side of the Alps, elongated, straight erosional scars that slope upward were assigned to a tunnel valley origin where subglacial meltwater under pressure substantially contributed to the incisions

* Corresponding author. Tel.: +41 31 6318771; fax: +41 31 6314843.
E-mail addresses: duerst@geo.unibe.ch (M. Dürst Stucki), schlunegger@geo.unibe.ch (F. Schlunegger).

0169-555X/$ – see front matter © 2011 Elsevier B.V. All rights reserved.
doi:10.1016/j.geomorph.2011.11.016

(Dürst Stucki et al., 2010; Jordan, 2010; Preusser et al., 2010). As many inner gorges in the Alps contain overdeepened segments (Pfiffner et al., 1997), a subglacial meltwater origin cannot be completely excluded.

Here, we propose a subglacial meltwater deepening of the *Lammschlucht* inner gorge located in the UNESCO Entlebuch area, central Switzerland. We combine detailed information about the morphometry of this gorge with a reconstruction of the glacial cover during the Last Glacial Maximum to infer hydrostatic erosion of this gorge. In particular, we use these data to calculate the hydraulic potential of basal meltwater in response to ice overburden patterns as the glacier crossed the gorge. These calculations yield distinct patterns of erosional potentials that are in line with the morphometric interpretation of the inner gorge. We support these calculations with shallow seismic data that illustrate substantial overdeepening along the same reach where the hydrologic model predicts the largest subglacial erosional potential.

2. Setting

The *Lammschlucht* hosts the Waldemme River that has its sources at the northern foothills of the Alps. It is a ca. 1600-m-long and >80-m-deep gorge with up to 60–80° steep bedrock valley flanks and is oriented toward the north (Fig. 1). The ca. 100–300 m-wide shoulders of this inner gorge are relatively flat and dip >40°, which in turn are bordered by soil-mantled hillslopes up to 25° steep. The bedrock is made up of conglomerates and sandstones and is exposed in some locations along the stream. The resulting cross section geometry displays a valley-in-valley cross section, which is a classical feature of most of the inner gorges in the Alps.

The study area is composed of a stack of Alpine thrust nappes (Fig. 2). In particular, the reach surrounding the *Lammschlucht* hosts three thrust sheets involving lower marine Molasse (LMM) and lower freshwater Molasse (LFM) deposits that are from north to south: (i) an early Miocene succession of alternating sandstone and mudstone beds several hundreds of meters thick that were formed by a meandering river. These deposits are overlain by (ii) the Beichlen thrust sheet with a <100 m-thick suite of shallow marine marls and sandstones at the base (LMM), and a >1000 m-thick alternation of late Oligocene conglomerates, sandstones and mudstones at the top (Diem, 1986; Mägert, 1998). The uppermost tectonic unit is referred to (iii) the Hilfern thrust sheet (LMM). It comprises an early Oligocene sandstone–mudstone alternation that was deposited by turbidity currents in an underfilled foreland trough (Diem, 1986). These units form a stack of imbricate thrust sheet that strikes NW–SE (Matter, 1964; Schlunegger et al., 1996). Accordingly, the incised gorge cuts the bedrock at a nearly right angle (Fig. 2). The upper termination of the *Lammschlucht* is located some hundreds of meters downstream of the thrust plane separating the sandstone–mudstone alternations of the Hilfern thrust sheet from the conglomerate–mudstone alternation of the Beichlen thrust sheet. At the end of the inner gorge, the valley widens at the stratigraphic contact between the shallow marine sandstone–mudstone alternation and the fluvial conglomerates (Fig. 2). The valley reaches the largest width where it is underlain by the early Miocene suite of sandstone–mudstone alternation.

During the Pleistocene, the area was repeatedly covered by glaciers and therefore experienced multiple phases of erosion and sediment accumulation in response to the glacial/interglacial cycles (e.g., Müller and Schlüchter, 1997; Schlunegger and Schneider, 2005). Upstream of the gorge, the trunk glacier was derived from the northern foothills of the Alps, from where it flowed across the ca. 1600-m-long gorge and then split into two branches, one in the direction of Entlebuch to the NE and one toward Schüpfheim to the SW (Fig. 3). As seen in the reconstructed ice cover and described in detail further below, the ice thickness substantially decreased immediately

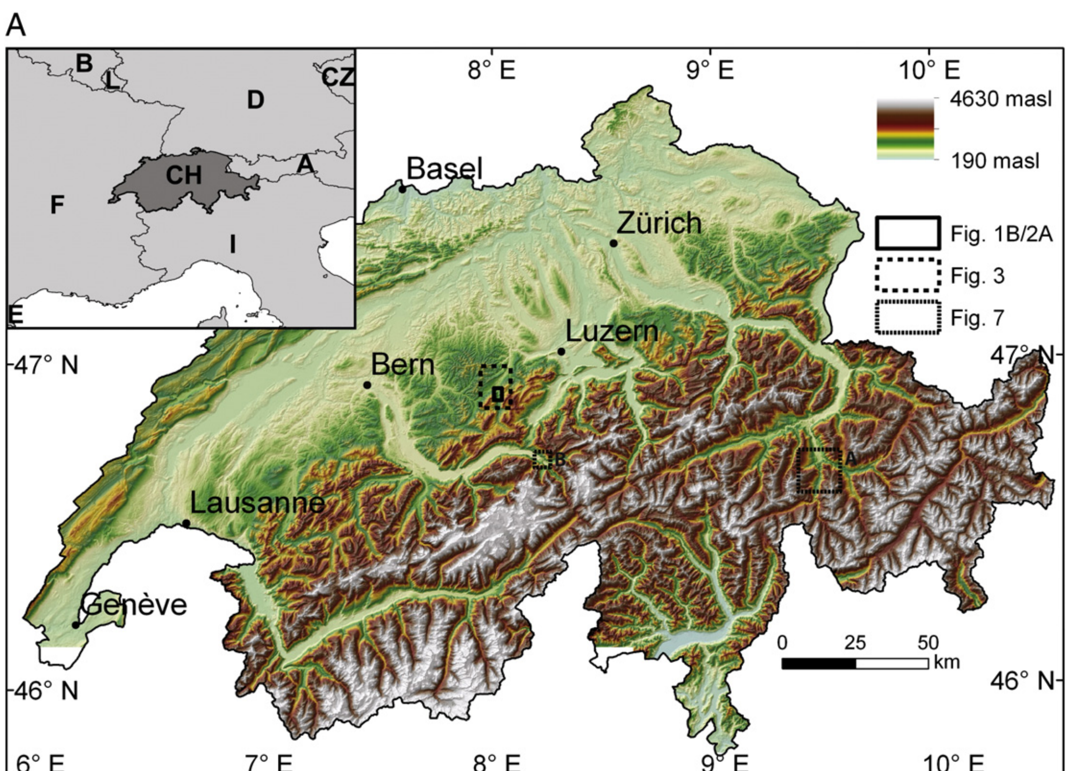

Fig. 1. (A) Overview figure illustrating the location of the *Lammschlucht* inner gorge in the UNESCO Entlebuch area, at the northern border of the Swiss Alps (black solid line). (B) The *Lammschlucht* inner gorge with its four segments: (i) upstream of the gorge, (ii) step-pool channel geometries, (iii) straight part with plane-bed channel morphologies, and (iv) downstream of the gorge where the Waldemme River represents a plane-bed geometry. The black circle represents the location of a borehole, where an overdeepening of 7.1 m was documented by the consulting company TerrBohr.

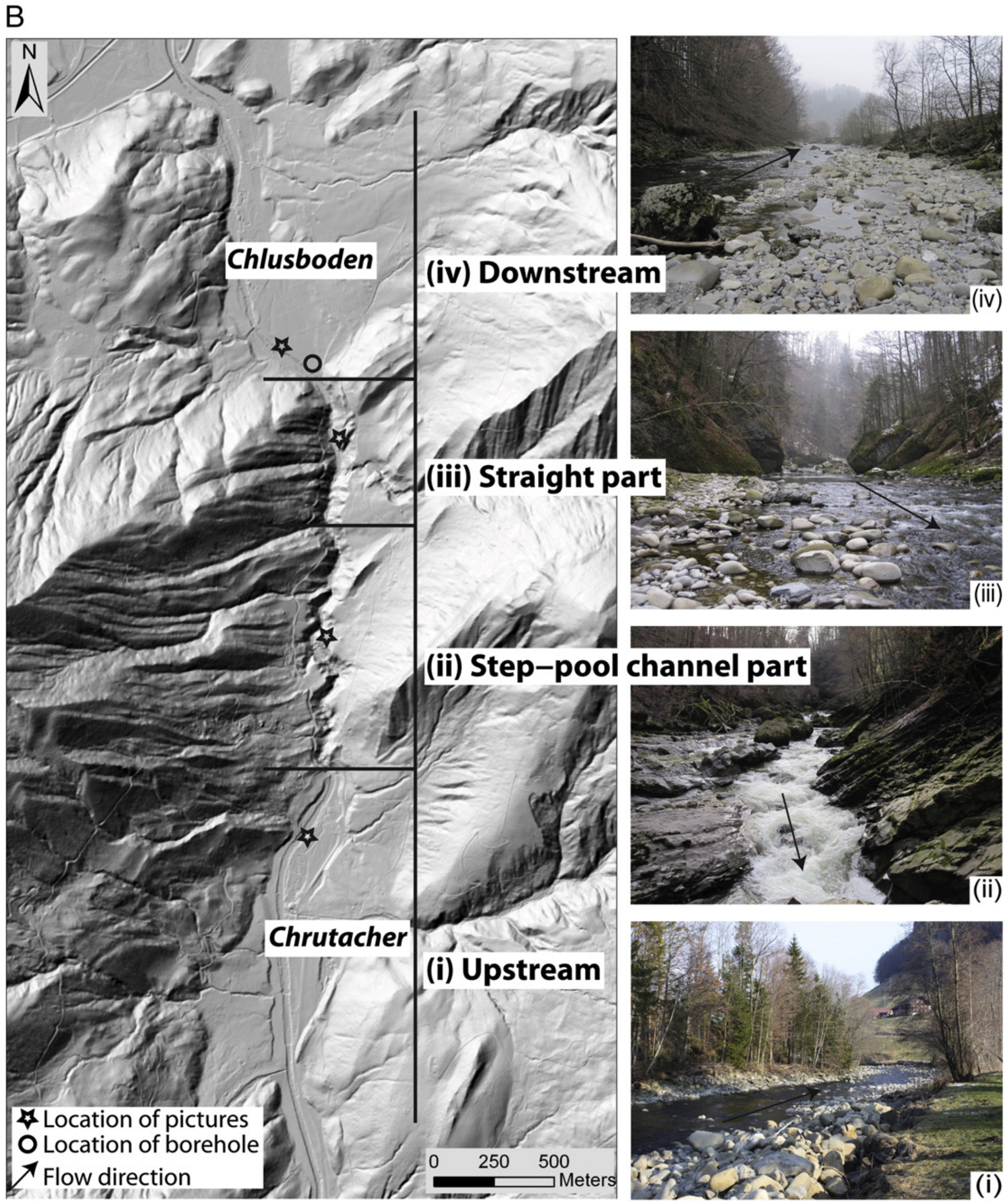

Fig. 1 (*continued*).

downstream of the gorge where the valley widens and the glacier split into two branches (Fig. 3C).

3. Methods

3.1. Channel morphology, and reconstruction of glacial cover

Following the scope of this paper, we first reconstructed the geomorphological properties of the *Lammschlucht* inner gorge by detailed mapping in the field. We identified the geomorphic properties of the channel and the bordering hillslopes, focusing particularly on the fabric of the channel floor.

As a next step in our analysis, we reconstructed a hypothetical glacial cover of the *Lammschlucht* area using lateral moraines and hanging talus cones that record the elevation of the ice surface. The maximum extent of the ice sheet during LGM times, including a restoration of the ice surface, was recently presented by Bini et al. (2009) (Fig. 3A). However, overpressurized water beneath the ice sheet has been shown to substantially contribute to erosion mainly during the deglaciation stages and beneath the equilibrium line altitude (ELA) (Brocklehurst and Whipple, 2002; Anderson et al., 2006; Herman and Braun, 2008; Egholm et al., 2009; Herman et al., 2011). Because of this, we reconstructed the ice surface based on evidence for deglaciation mechanisms. Upstream of the inner gorge, lateral moraines, hanging tributary fans, and streamline forms of bedrock knobs indicative of glacial polishing are used to reconstruct the elevation of the glacier surface during late LGM time (Fig. 3B). For instance, colluvium deposits at elevations higher than 1100 m asl are frequently observed upstream of the incised gorge, where they form hanging fans several tens of meters thick with lateral extents ranging between tens to hundreds of meters. The bedrock at and beneath these elevations displays streamline forms with convex-up curvatures that are tens to hundreds of meters long. These bedrock knobs reveal a direction that parallels the bedding orientation of the bedrock, which

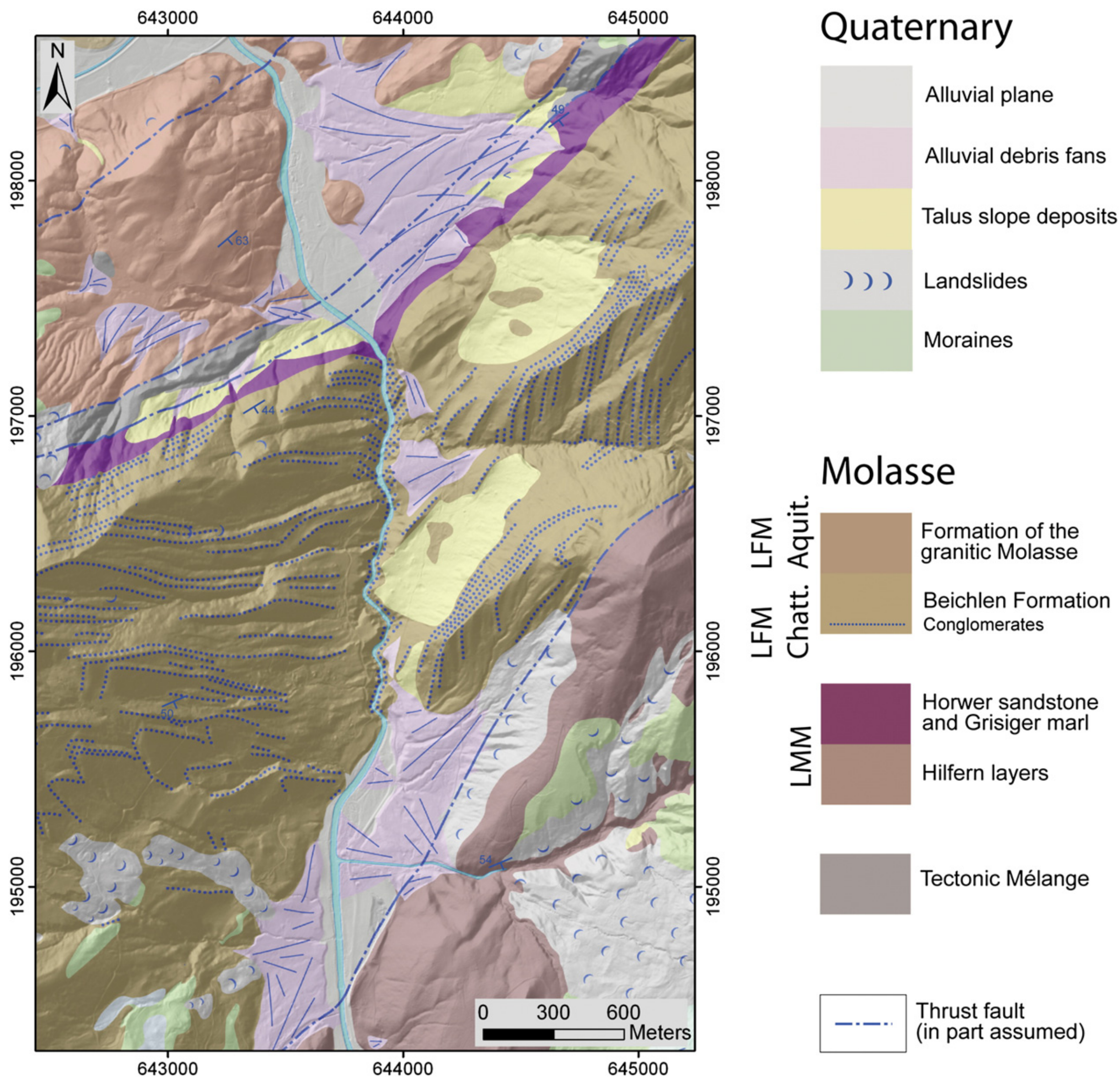

Fig. 2. Geological map of the *Lammschlucht* area. The bedrock geology comprises lower marine Molasse (LMM) and lower freshwater Molasse (LFM) groups: (i) the Early Oligocene Hilfern thrust sheet made up of sandstone–mudstone alternations; (ii) the Late Oligocene Beichlen thrust sheet with alternated conglomerate, sandstone, and mudstone beds; and (iii) the early Miocene succession of sandstone and mudstone beds.

indicates glacial carving of bedrock. The knobs are also covered by a meter thick regolith of fine-grained unconsolidated material. We used the highest elevation of these geomorphic features to reconstruct the ice surface.

We likewise paid special attention on the careful reconstruction of the ice sheet within and downstream of the inner gorge because subglacial meltwater potentially contributes to erosion not only around the ELA (located near the reach of the inner gorge) where the ice sliding velocity is usually fastest, but also in the ablation area as revealed by numerical models (Brocklehurst and Whipple, 2002; Anderson et al., 2006; Herman and Braun, 2008; Egholm et al., 2009; Herman et al., 2011). Accordingly, downstream of the inner gorge, a well-developed suite of down-dipping lateral moraines at successively lower elevations between Schüpfheim and Hasle immediately downstream of the incised gorge (Mollet, 1921) (Fig. 3B) is indicative of a downmelting glacier. We used the highest of these deglacial features for our reconstruction (Fig. 3B).

However, major uncertainties in the reconstruction of the ice surface and thus the ice thickness in the region of the gorge result from a lack of constraint for the curvature of the ice, particularly in the middle of the glacier. This lack of a robust methodology to reconstruct the paleo-ice surface is well known. Ng et al. (2010) identified further uncertainties related to poorly constrained data regarding basal sliding mechanisms, anisotropy in ice rheology, and unknown ages of related deposits such as lateral and frontal moraines, which is the case here as well. We proceeded by (i) linking identical elevations with contour lines yielding a constant curvature and (ii) selecting a minimum curvature difference between neighboring contour lines. This approach is justified through the plastic material properties of ice that tend to result in a smoothing effect and thus in contour lines with nearly constant curvatures and in the generally convex form of modern glacial surfaces beneath the ELA (Nye, 1952).

Nevertheless, any deviations from the concepts that we applied will not alter the observation of a rapid decrease in ice thickness where the valley widens near the end of the inner gorge (see below).

3.2. Modeling of subglacial hydrology

The reconstruction of the ice cover map then allowed us to calculate the hydraulic potential gradients of the water at the base of a

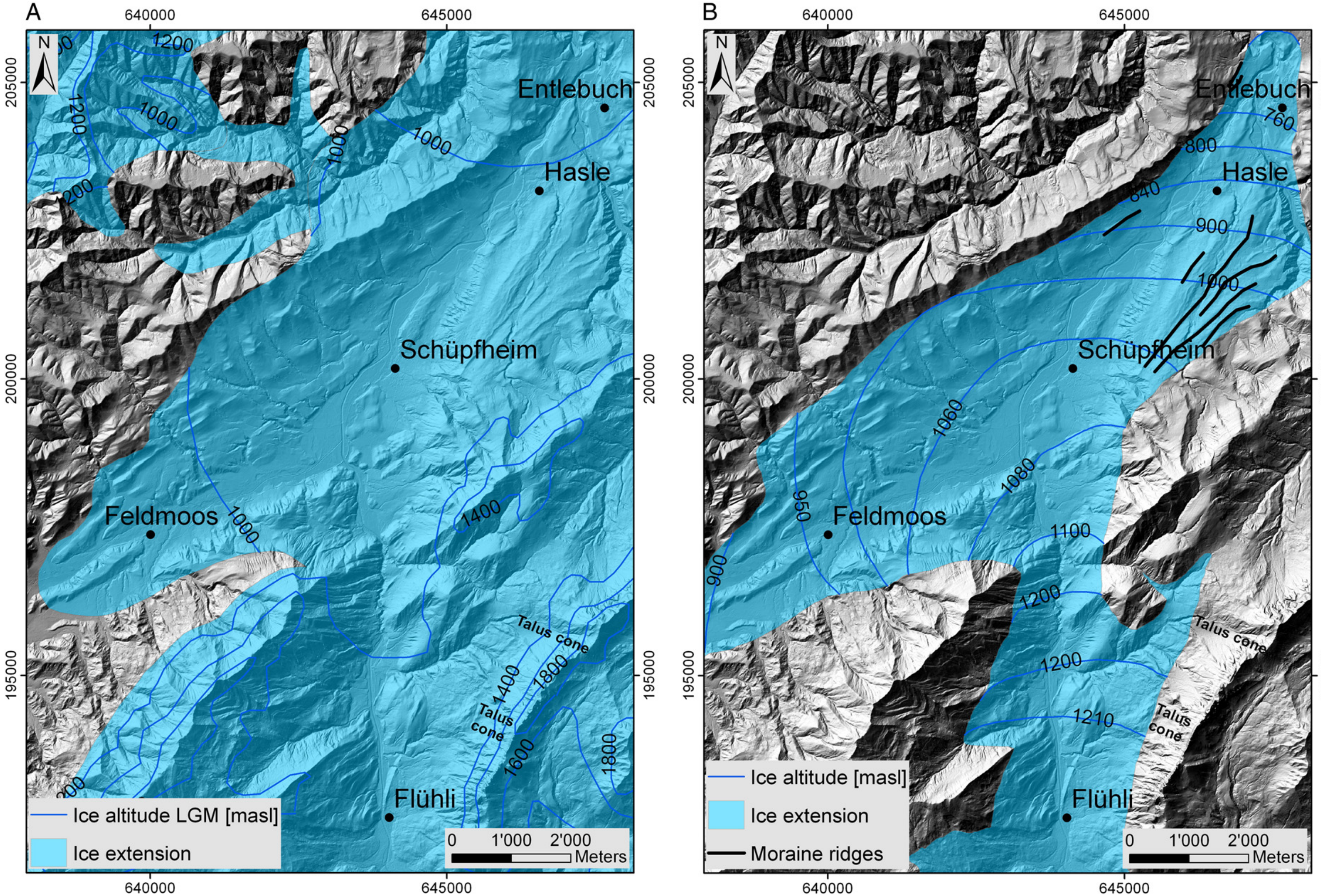

Fig. 3. (A) Glacial cover during the period of the maximum extent during the Last Glacial Maximum (LGM) at around 21 ka (after Bini et al., 2009). (B) Restored glacial cover during deglaciation of the Last Glacial Maximum (LGM). Lateral moraines and hanging talus cones that record the elevation of the ice surface at one particular stage during the LGM were used to restore a glacial cover that most likely represents a deglaciation stage. (C) Thickness of the restored glacial cover. The decrease of ice thickness downstream of the inner gorge is visible. The calculation is based on today's topography.

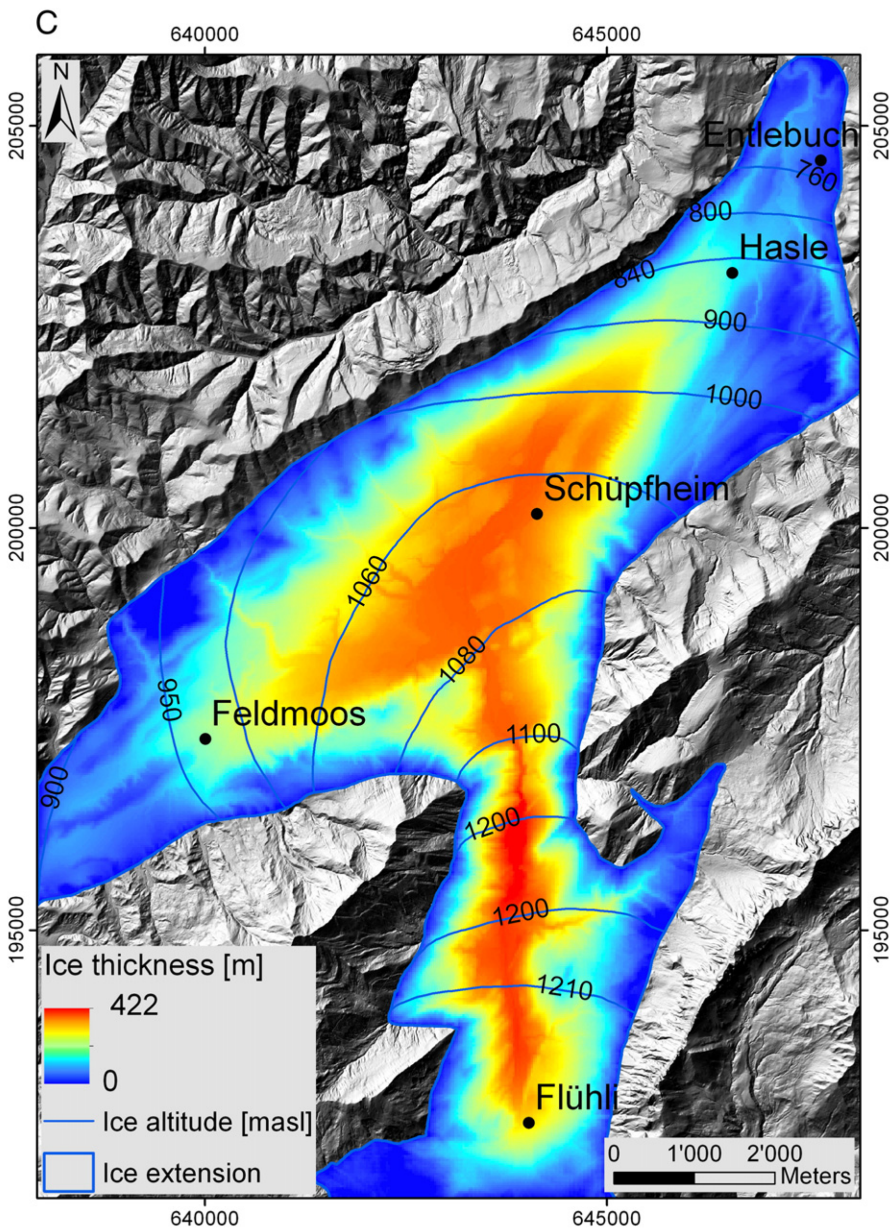

Fig. 3 (*continued*).

glacier, which likewise can be used as a proxy for the erosional potential of the meltwater beneath the ice. According to Shreve (1972) this hydrological potential is equal to

$$\phi_b = P_w + \rho_w g z_b \tag{1}$$

where $P_w = k\rho_i g(z_s - z_b)$ is the subglacial water pressure, ρ_w and ρ_i are the densities of water and ice (respectively), g is the acceleration caused by gravity, z_b is the elevation of the glacier bed, z_s is the elevation of the ice surface and k is a factor between 0 and 1 representing the range of the subglacial water pressure from atmospheric pressure ($k = 0$) to full ice-overburden pressure ($k = 1$) (Shreve, 1972; Sugden et al., 1991; Fischer et al., 2005).

According to the conservation of energy, changes in the hydrological potentials are transferred into a corresponding shift in the dynamic pressure, which likewise is a measure of the erosional potential (Koppes and Montgomery, 2009). In the case of a hydrologically closed system, the sum of the static, geodetic, and dynamic pressures is constant and is equal to

$$p + \frac{1}{2}\rho v^2 + \rho g h = p_{tot} = cte \tag{2}$$

where p is the pressure, ρ is the water density, v is the velocity of water, h is the elevation of the glacier bed, and g is the gravitational acceleration. The term p then reflects the static pressure (equal to the first term in Eq. (1)), 1/2 ρv^2 the dynamic pressure, and ρgh the geodetic pressure (equal to the second term in Eq. (1)). Eq. (2), which is referred to as the Bernoulli solution for the conservation of hydrological energy, can then be solved for flow velocity, which likewise is a measure of the erosional potential (Koppes and Montgomery, 2009). We then calculated the static and the geodetic pressures according to Eq. (1) along the thalweg using the restored ice thickness pattern and the elevation of the Waldemme River as the basis. These two pressure components allowed us to identify the changes of the dynamic pressure along the stream.

Because the Bernoulli equation applies for a hydrologically closed system only, we assumed the Lammschlucht inner gorge as closed system for simplicity. We calculated this equation for two steady-state conditions in a temperate glacier. The first approach considered a value of $k=1$ where the water pressure equals the ice-overburden pressure. We then set the value $k=0.5$ during a second calculation run, which corresponds to a situation where the water pressure may drop below the ice-overburden pressure as a consequence of open crevasses or the development and enlargement of drainage channels beneath the glacier (Fischer et al., 2005). We acknowledge that this approach bases on the assumption of a steady water flow, which deviates from the observation of meltwater pulses. However, also in this latter scenario, pulses that release subglacially stored water can be related to pressure gradients and are likewise considered to contribute to the enlargement of conduits (Sjogren et al., 2002; Clarke et al., 2005).

3.3. Measurement of glacial overdeepening at the downstream end of the gorge

We determined the depth of potential overdeepening at the end of the gorge based on a refraction seismic survey. The measurements were performed during dry weather conditions immediately following two days of rain (total of approx. 10 mm). We measured two roll-along sections with total line lengths of 215 m and 246 m, respectively (Fig. 1B). The SW–NE oriented Section 1 runs perpendicular to Section 2 and comprises two single surveys with a length of 115 m each (24 recorders, 5 m spacing) overlapping by 15 m (Fig. 5). The NW–SE oriented Section 2 runs parallel to the Waldemme River and consists of three single surveys with a length of 115 m each (24 recorders, 5 m spacing) and two overlaps of 80 m and 20 m (Fig. 5). The signal was triggered with a 5 kg sledge hammer at each recorder position with a lateral offset of 50 cm. This resulted in a total number of 48 and 72 shots. We stacked each shot five times in order to improve the signal to noise ratios. Geophone positions were determined with a differential GPS.

We processed the seismic data with *ReflexW* (Sandmeier Scientific Software). We started with an initial model of subsurface conditions that is based on a wave-front inversion of assigned traveltimes. The final three layer model was then created by forward modeling using the network raytracing method. Model fit was optimized visually through comparison between the data traveltimes and the calculated traveltimes, as well as numerically by means of diminishing RMS deviations finally yielding values of 2.39 (Section 1), and 2.66 (Section 2).

4. Results

4.1. Channel morphology, and reconstruction of glacial cover

Upstream of the gorge, the entire valley is >4 km wide where it is underlain by the sandstone–mudstone alternation of the Hilfern thrust sheet. Here, the channel floor displays a <2-m-thick cover of pebbles and gravels, and the bedrock of the Hilfern unit is exposed in places particularly where it comprises sandstone and conglomerate interbeds. The valley width then decreases to ca. 3 km where the gorge is cut into the Oligocene conglomerate–mudstone alternation and reaches a minimum width of ca. 2.5 km near the downstream end of the incised reach. The inner gorge has two distinct segments that contrast in channel geometries: a meandering step-pool and a straight channel part (Fig. 1B). In the uppermost ca. 1000-m-long reach of the inner gorge, the channel floor exposes the Oligocene bedrock. It displays a step-pool morphology (Montgomery and Buffington, 1997; Whipple, 2004) and meanders around the SE–NW striking, 5–10 m-thick conglomerate beds where conglomerate tops form ca. 2-m-high bedrock steps (Fig. 1B). Also in this uppermost reach, the bedrock has streamline forms and vertical cavities with diameters ranging between 1 and 2 m. Along the subsequent lower 600-m-long segment (Fig. 1B), the channel has a straight course; and the floor is covered by a several meter thick sheet of gravel derived from farther upstream and conglomerate blocks up to several cubic meters large that originated from bank collapse. The channel then widens from <5 to >10 m near the mouth of the gorge where lateral and longitudinal gravel bars that are up to 10 m long are more frequent. Bedrock steps are absent in this lowermost reach. This lower straight channel segment can be described as plane-bed type according to the classification by Montgomery and Buffington (1997).

Farther downstream immediately at the outlet of gorge where the bedrock changes to shallow marine marls and Miocene sandstone–mudstone alternations of fluvial origin (Fig. 2), the valley floor widens from 10 to >300 m over a distance of a few meters (Fig. 1B). Here, borehole and seismic data (Fig. 5, see below) reveal that the bedrock is covered by a 6–7-m-thick succession of unconsolidated fluvial gravels and boulders, pointing toward the presence of an overdeepened segment. The bedrock then crops out on the channel floor ca. 1000 m farther downstream of the gorge mouth where the channel is confined in a ca. 5-m-wide passage bordered by glacially sculpted bedrock knobs (Fig. 2).

The reconstructed map of the glacial cover is presented in Fig. 3. It shows that the ice surface was nearly flat upstream of the inner gorge where the surface elevation dropped from 1210 m asl to 1200 m asl over a ca. 2000-m-long reach. However, in the lower segment of the gorge and immediately downstream of the *Lammschlucht* inner gorge where the valley widens, our reconstruction implies a rapid elevation drop of the ice surface from 1200 to 1080 m asl over a distance of 2000–2500 m. Farther downstream, well-developed lateral moraines indicate elevations beneath the ELA where the ice surface elevation finally decreased to ca. 760 m asl. Note that our reconstructed glacial cover differs from the map of the LGM, which illustrates the maximum extent of the glaciers at around 21 ka (Fig. 3) (Bini et al., 2009). In particular, our reconstructed contour lines display a convex form, which differs from the reconstruction during the maximum extent of the LGM glaciers because of the shift of the ELA to a higher elevation during deglaciation (Nye, 1952).

4.2. Modeling of subglacial hydrology

The results of the hydrological calculations that are based on Eq. (2) are shown in Fig. 4A. The resulting pressures are normalized to a range between 0 and 100 for intercomparison and smoothed. A further motivation for the selection of this approach is the lack of standardized dynamic pressure data, which precludes the calculation of effective values of the dynamic pressure. Nevertheless, because of the linear nature of Eq. (2), the normalization of the values allows us to calculate the effective downstream changes of the pressures within the inner gorge. The results reveal a continuous decrease of the geodetic pressure along the thalweg. In contrast, the static pressure rises in the downstream direction. It reaches a maximum in the step-pool channel part (section (ii) of Fig. 1B), and then drops to a minimum at the end of the *Lammschlucht* due to the decrease of the ice thickness. The combination of both pressure components through Eq. (2) implies a continuous increase of the dynamic pressure toward the end of the inner gorge where it reaches maximum values.

Fig. 4B shows the difference between the calculations when different k-values are considered. The first approach was achieved with a value of $k=1$, i.e., the subglacial water pressure equals the ice-overburden pressure. For the second calculation, we used a value of $k=0.5$, i.e., the subglacial water pressure may drop below the ice-overburden pressure. This corresponds to the situation when the hydrological system beneath the ice sheet was not closed, i.e., when pathways impede the full downstream transformation of hydraulic potential. The dynamic pressure is then slightly enhanced in the calculation with a value of $k=0.5$. This is because of meltwater input or the development and enlargement of drainage channels beneath the glacier either by continuous flows, or

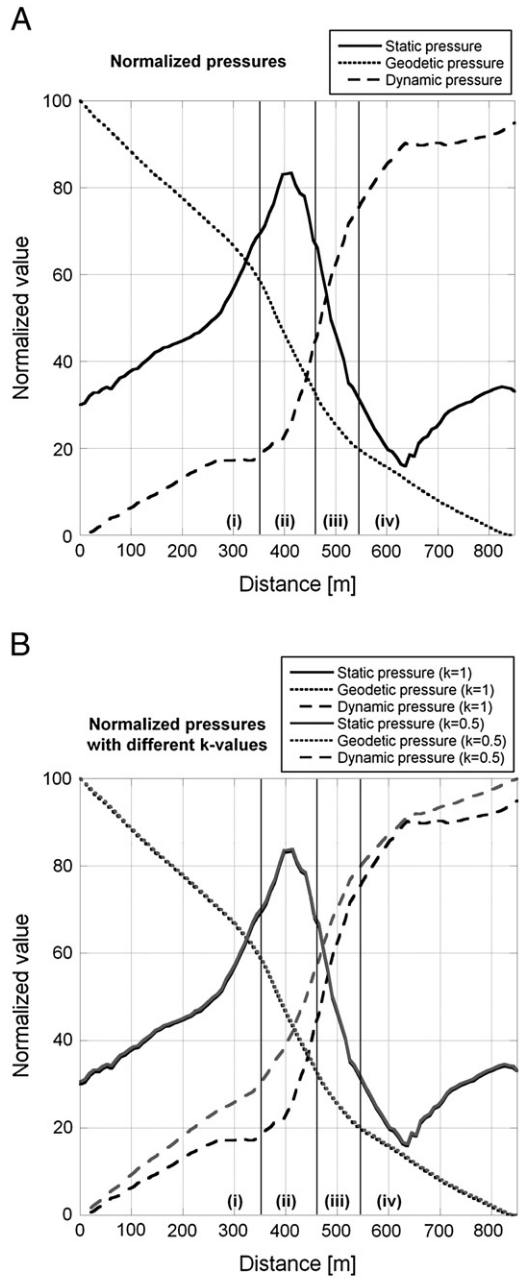

Fig. 4. (A) The calculated pressure in the *Lammschlucht*. The labels (i)–(iv) mark the different sections within the inner gorge (see Fig. 1B). The calculations imply that the dynamic pressure (dashed line) rises toward the end of the inner gorge mainly because of changes of ice thickness. (B) The calculated pressure in the *Lammschlucht* with the two different *k*-values (see text for further information). The dynamic pressure is slightly enhanced in the calculation with a value of k = 0.5.

by meltwater pulses (Sjogren et al., 2002). As a consequence, the erosion potential is slightly higher when this latter situation is considered because of the enhanced flow velocity.

4.3. Measurement of glacial overdeepening at the downstream end of the gorge

The analysis of the seismic data is guided by the consideration of the local topographic situation (floodplain and shallow, glacially scoured basin) and the preceding weather situation (intense rain fall). Accordingly, we restored a three layer model of the subsurface (Fig. 5) that comprises: (i) an uppermost layer with velocities between 200 and 500 m/s, (ii) a second medium-velocity layer with seismic velocities of 1400 m/s, and (iii) a lowermost third layer with a velocity of 2600 m/s. We interpret the uppermost unit as fluvial gravel deposits with a high content of groundwater and an organic rich soil on top. The underlying second unit most likely reflects the presence of glaciofluvial and fluvial deposits with a high water content. The bottom third layer with the highest velocity is considered as the bedrock surface that is present here by alternated sandstones and marls of the Miocene lower freshwater Molasse. Our interpretation is guided by nearly identical wave propagation velocities that were published for sandstone–mudstone alternations in the eastern Molasse (1800–3500 m/s, Knödel et al., 1997).

The geometry of Section 2 suggests that the bedrock surface drops sharply in close proximity to the exit of the gorge toward a maximum depth of around 7 m. This depth corresponds to the drilling located on Section 2 (meter 213) which reached the bedrock at a depth of 7.1 m. The seismic data of Section 1 that runs perpendicular to the valley orientation (and thus to Section 2) reveals a similar subsurface architecture including a 1–1.5 m-thick topsoil and unsaturated gravels, a ca. 5–6 m-thick suite of glaciofluvial and fluvial gravels, and the bedrock underneath.

5. Discussion and conclusion

Montgomery and Korup (2011) proposed that the formation of inner gorges in the Swiss Alps probably started prior to the LGM. These authors based their interpretation on erosion rate budgets, indicating that the average erosion rates for an exclusively post-glacial gorge cutting are inconsistent with long-term exhumation rates in the Alps. We propose here a mechanism by which the *Lammschlucht* inner gorge has formed and evolved through time. In particular, we consider that pressurized meltwater during deglaciation stages resulted in the deepening of the gorge particularly in the lower reach of the *Lammschlucht* where ice thickness decreased over short distances in response to valley widening (Fig. 3). We base this interpretation on the results of our simple hydrological model paired with observations in the field. We then discuss the controls of the underlying lithology on the large-scale topographic architecture of the entire valley and outline how mechanical contrasts of bedrock constrain the ice flow, which in turn has implications for hydraulic potential beneath the glacier. This lithological architecture may also have resulted in deepening of the gorge during previous glaciations, as detailed below. Finally, we will present two further not yet explored but well known examples where subglacial meltwater could have influenced the formation of inner gorges.

5.1. Subglacial meltwater and erosional scouring

We use calculations of hydraulic potentials in the *Lammschlucht* to infer the controls of overpressurized meltwater on valley deepening during, presumably, the deglaciation. In particular, as seen in Fig. 4, the dynamic pressure is highest at the end of the inner gorge, thus resulting in a maximum value of the erosional potential. This is also the reach where the underlying bedrock changes from conglomerate–mudstone alternations with presumably medium erodibility to a suite of sandstones and mudstones that have a high erodibility according to Kühni and Pfiffner (2001) (Fig. 2). This situation, where the inferred highly erosive meltwater flows over bedrock with low erosional resistance, most likely resulted in the scouring of a depression in the Chlusboden area downstream of the *Lammschlucht* (Fig. 5). The observation of depressions with concave-up long profiles indicates that the scouring occurred through pressurized, subglacial water (Sjogren et al., 2002). Consequently, we propose that the inner gorge in the Waldemme River deepened to a large extent as a consequence of subglacial meltwater erosion rather than fluvial erosion (Fig. 6). During interglacial times,

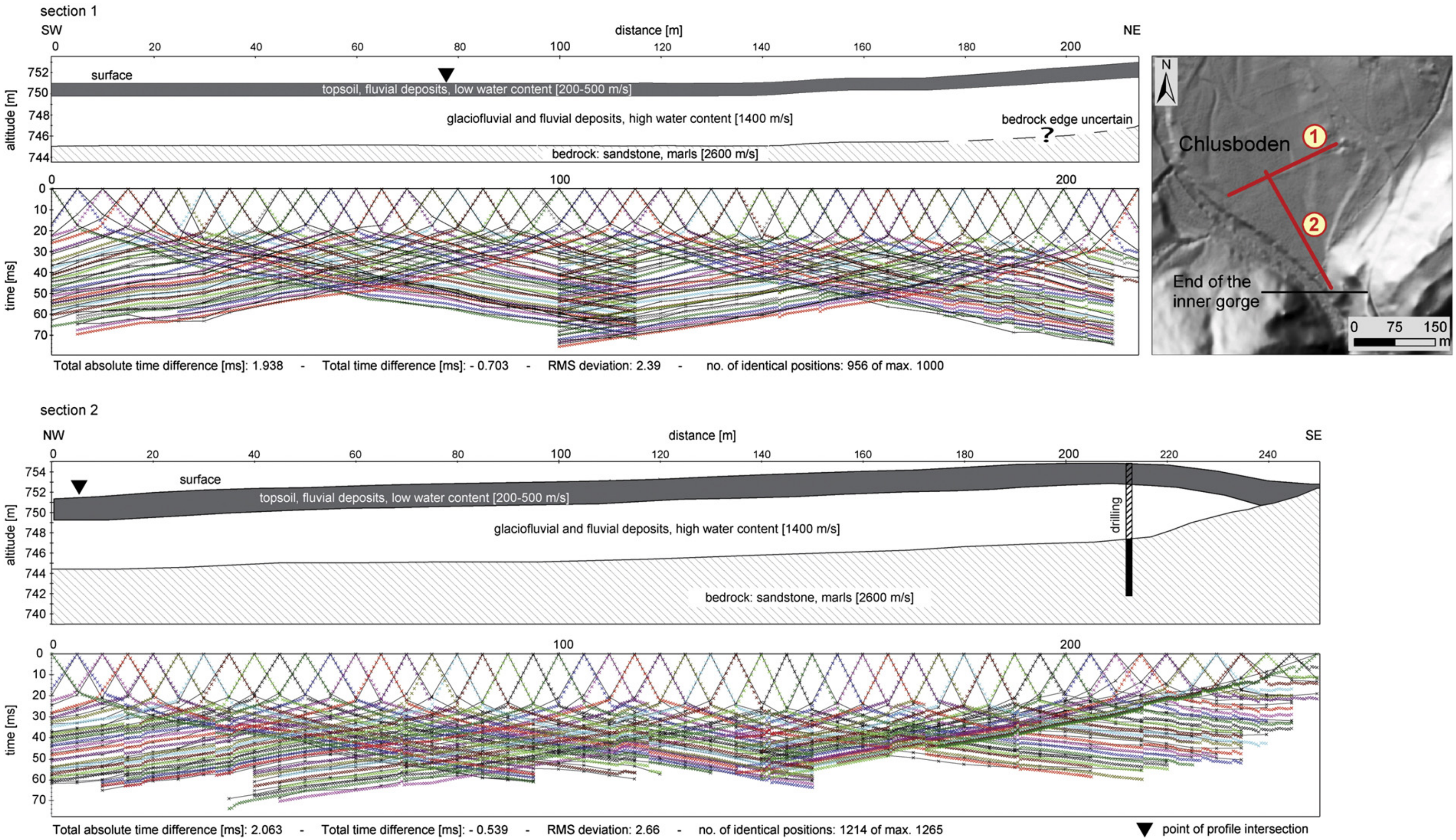

Fig. 5. The analysis of the seismic data shows a depth of the bedrock surface in the Chlusboden area of about 6–7 m below the surface.

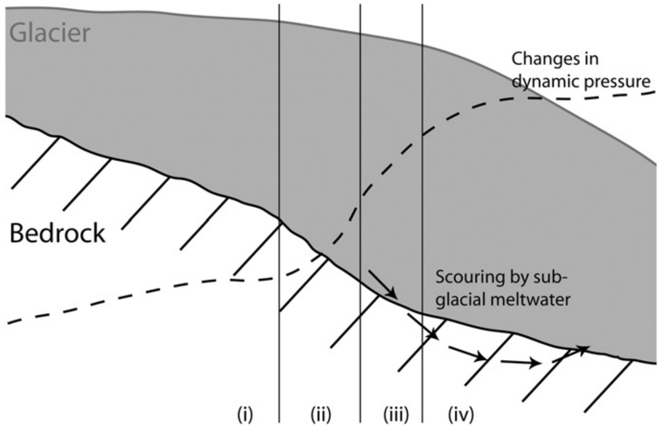

Fig. 6. Schematic geomorphic model of the scouring at the end of the inner gorge by subglacial meltwater. The black arrows represent the hypothetical erosion of the meltwater from the enhanced dynamic pressure.

the scoured depression was refilled by fluvial gravels, which currently form the longitudinal bars in the lower straight segment of this inner gorge (segment (iii) in Fig. 1B). The situation, however, is different in the upper segment of the inner gorge where step-pool channel morphologies prevail (segment (ii) in Fig. 1B). Here, streamline forms point toward fluvial abrasion by bedload and suspension load, which in turn is indicative of ongoing downcutting and regressive erosion in the channel. Accordingly, the current state of adjustment in present times is situated in the upper segment of the inner gorge and ends where the step-pool channel part changes into a straight river flow (boundary between sections (ii) and (iii) in Fig. 1B).

As seen in Fig. 4B, a slight difference occurs between the calculations when different k-values are considered. In particular, the dynamic pressure with $k = 0.5$ is enhanced compared to the situation where $k = 1$. This implies an increase in the flow velocity for the situation where surface meltwater was additionally supplied to the water flow beneath the ice (see above). Accordingly, an open system could have resulted in a positive feedback where a supply of supraglacial and englacial water resulted in the development and enlargement of drainage channels beneath the glacier. Accordingly, this increase of channelization would additionally contribute to the focusing of the erosion in the subglacial drainage channels (Sjogren et al., 2002). In addition, a higher subglacial water discharge, mainly during deglaciation stages, plays a significant role in 'glacial processes' (Eyles, 2006). Indeed, enhancements of erosion rates during deglaciation have been observed by different authors (e.g., Koppes and Hallet, 2002, 2006; Koppes and Montgomery, 2009). In particular, the higher amount of basal water influences the stress distribution at the glacier bed and leads to higher sliding velocity of the ice and thus to higher erosion rates (e.g., Iken and Bindschadler, 1986; Fountain and Walder, 1998; Alley et al., 1999; MacGregor et al., 2000; Koppes and Montgomery, 2009). In a recent paper, Herman et al. (2011) modeled glacial erosion via the reconstruction of ice flow and the integration of subglacial hydrology. They showed that subglacial hydrology has fundamental impacts on the temporal and spatial patterns of glacial erosion and therefore on the formation of overdeepenings and steps. Their overall conclusion where enhanced meltwater during deglaciation stages results in higher sliding velocities and thus higher erosion rates is in line with our inferred mechanisms. We additionally postulate that a substantial contribution of this mechanism can be related to the erosional effect of subglacial meltwater alone, which finally results in the deepening of inner gorges. This meltwater contribution to erosion can either occur as a steady process where the flow is continuous, or as erosional response to outbursts of meltwater that release subglacially stored water from overpressure (Sjogren et al., 2002; Clarke et al., 2005).

5.2. Lithology controls

Our simple hydrological model reveals that the decrease in ice thickness downstream of the inner gorge substantially contributes to the enlargement of the dynamic pressure and thus to an acceleration of the erosional potential. This decrease of the ice thickness is ultimately linked to the downstream changes of bedrock lithologies. In particular, the Oligocene conglomerates with inferred, relatively high erosional resistance resulted in restrictions for the flowing ice. In the case where the ice flux is constant in the downflow direction,

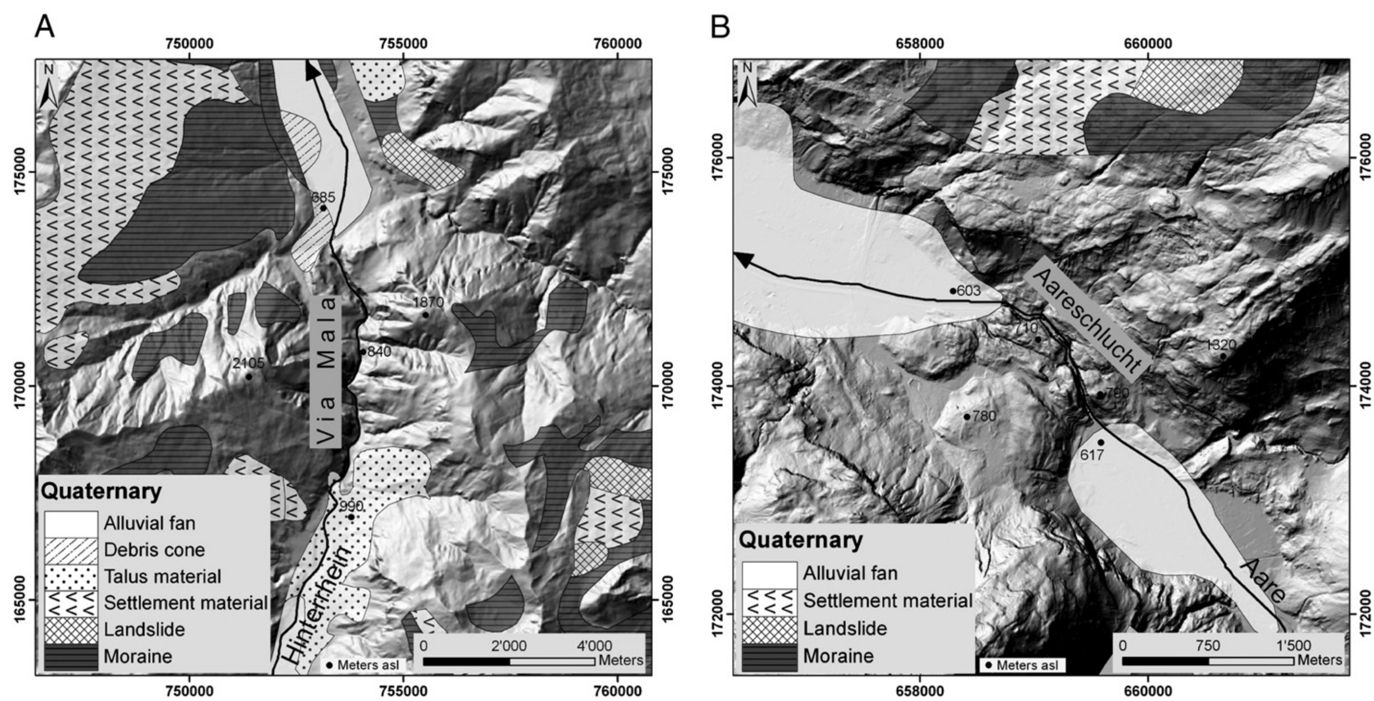

Fig. 7. Hill-shaded DEM of the (A) the *Via Mala* and (B) the *Aareschlucht* gorges, which might have the same genesis history as the *Lammschlucht*. Both of these inner gorges host a deep and narrow valley and are characterized by valley narrowing and opening in the downstream direction.

which we anticipate was the case, then any changes in cross-sectional valley widths will ultimately be compensated by corresponding adjustments of ice thickness through plastic flow (conservation of mass). We use these mechanisms to explain why the reconstructed elevation of the ice surface was nearly constant in the inner gorge reach and then decreased by ca. 100 m toward the lower end of the gorge over relatively short distances of a few hundreds of meters (Fig. 3B). The effect is a substantial decrease of the ice pressure and thus of the static pressure, which likewise could be transferred into a higher dynamic pressure according to Eq. (2) (Fig. 4). We thus interpret that the Oligocene conglomerates caused flow constrictions also during earlier glaciations and thus postulate multiple phases of scouring and redeposition in response to glacial–interglacial cycles.

5.3. Implications for other inner gorges in the Alps

The *Via Mala* in the Grisons Alps and the *Aareschlucht* in the Bernese Alps (Fig. 7) are two famous examples of deeply incised gorges (Buxtorf, 1919; Hantke and Scheidegger, 1993). Interestingly, the geomorphological architecture is identical to the situation at *Lammschlucht*. In particular, these gorges are characterized by valley narrowing in the downstream direction and by subsequent widening of the cross-sectional widths by several hundreds of meters. Their similarity to the *Lammschlucht* implies that they were deepened by subglacial meltwater under pressure. Consequently, we anticipate that other sites where a wide valley experiences constrictions in width and then widens again might have been shaped to a large extent by pressurized water underneath Alpine glaciers.

We conclude that presumably many inner gorges in the Alps record the combined effect of subglacial meltwater during glaciations, and fluvial processes during interglacial stages. Whereas meltwater erosion is mainly seen in deep scouring at the downstream end of these inner gorges, fluvial downcutting during subsequent interglacial times has deepened these gorges predominantly in the upstream reach. These mechanisms, one operating during glacial times and the other during interglacial periods, have not been investigated in sufficient details and warrant further studies.

Acknowledgments

This paper greatly benefited from helpful feedbacks from Kevin Norton and Urs H. Fischer. We thank Bernhard Salcher as reviewer and Richard Marston as editor for their constructive comments and suggestions. The project was supported by the Swiss National Science Foundation (SNF, 20TO21-120525), and the ESF TopoEurope Project.

References

Ahnert, F., 1988. Modelling landform change. In: Anderson, M.G. (Ed.), Modelling Geomorphological Systems. Wiley, New York, NY, pp. 375–400.
Alley, R.B., Strasser, J.C., Lawson, D.E., Evenson, E.B., Larson, G.J., 1999. Glaciological and geological implications of basal-ice accretion in overdeepenings. In: Mickelson, D.M., Attig, J.W. (Eds.), Glacial Processes Past and Present. Geological Society of America Special Paper. Geological Society of America, Boulder, CO, pp. 1–9.
Anderson, R., Hallet, B., Raymond, C., 2006. Features of glacial valley profiles simply explained. Journal of Geophysical Research 111, F01004.
Bini, A., Buoncristiani, J.-F., Couterrand, S., Ellwanger, D., Felber, M., Florineth, D., Graf, H.R., Keller, O., Kelly, M., Schlüchter, C., Schoeneich, P., 2009. Die Schweiz während des letzteiszeitlichen Maximums (LGM) 1:500'000. Bundesamt für Landestopografie Swisstopo, Switzerland.
Bonnet, S., Bernard, M., Driessche, J.V., 2001. Drainage network expansion of the Salagou drainage basin (S. France): an example of relief response to recent climate change? Terra Nova 13, 214–219.
Brocklehurst, S.H., Whipple, K.X., 2002. Glacial erosion and relief production in the eastern Sierra Nevada, California. Geomorphology 42, 1–24.
Buxtorf, A., 1919. Aus der Talgeschichte der ViaMala. Vierteljahrsschrift der Naturforschenden Gesellschaft in Zürich 64, pp. 434–456.
Cadisch, J., 1926. Zur Talgeschichte von Davos. Jahresbericht der Naturforschenden Gesellschaft Graubünden 59, 285–299.
Clarke, G.K.C., Leverington, D.W., Teller, J.T., Dyke, A.S., Marshall, S.J., 2005. Comments to Paleohydraulics of the last outburst flood from glacial Lake Agassiz and the 8200 BP cold event. Quaternary Science Reviews 24, 1533–1541.
De Graaff, L.W.S., 1996. The fluvial factor in the evolution of alpine valleys and of ice-marginal topography in Vorarlberg (W-Austria) during the upper Pleistocene and Holocene. Zeitschrift für Geomorphologie 104, 129–159.
Densmore, A.L., Hovius, N., 2000. Topographic fingerprints of bedrock landslides. Geology 28, 371–374.
Densmore, A.L., Anderson, R.S., McAdoo, B.G., Ellis, M.A., 1997. Hillslope evolution by bedrock landslides. Science 275, 369–372.
Diem, B., 1986. Die untere Meeresmolasse zwischen der Saane (Westschweiz) und der Ammer (Oberbayern). Eclogae Geologicae Helvetiae 79, 493–559.
Dürst Stucki, M., Reber, R., Schlunegger, F., 2010. Subglacial tunnel valleys in the Alpine foreland: an example from Bern, Switzerland. Swiss Journal of Geosciences 103, 363–374.
Egholm, D., Nielson, S.B., Pedersen, V.K., Lesemann, J.E., 2009. Glacial effects limiting mountain height. Nature 460, 884–887.
Eyles, N., 2006. The role of meltwater in glacial processes. Sedimentary Geology 190, 257–268.
Fischer, U.H., Braun, A., Bauder, A., Flowers, G.E., 2005. Changes in geometry and subglacial drainage derived from digital elevation models: Unteraargletscher, Switzerland, 1927–1997. Annals of Glaciology 40, 20–24.
Fountain, A.G., Walder, J.S., 1998. Water flow through temperate glaciers. Reviews of Geophysics 36, 299–328.
Hantke, R., Scheidegger, A.E., 1993. Zur Genese der Aareschlucht. Geographica Helvetica 48, 120–124.
Herman, F., Braun, J., 2008. Evolution of the glacial landscape of the Southern Alps of New Zealand: insights from a glacial erosion model. Journal of Geophysical Research 113, F02009.
Herman, F., Beaud, F., Champagnac, J.D., Lemieux, J.M., Sternai, P., 2011. Glacial hydrology and erosion patterns: a mechanism for carving glacial valleys. Earth and Planetary Science Letters 310, 498–508.
Iken, A., Bindschadler, R.A., 1986. Combined measurements of subglacial water pressure and surface velocity of Findelengletscher, Switzerland: conclusions about drainage system and sliding mechanism. Journal of Glaciology 32, 101–119.
Jordan, P., 2010. Analysis of overdeepened valleys using the digital elevation model of the bedrock surface of northern Switzerland. Swiss Journal of Geosciences 103, 375–384.
Kelsey, H.M., 1988. Formation of inner gorges. Catena 15, 433–458.
Knödel, K., Krummel, H., Lange, G., 1997. Geophysik. Handbuch zur Erkundung des Untergrundes von Deponien und Altlasten. Springer-Verlag, Berlin, Germany, p. 1063.
Knudsen, Ó., Marren, P.M., 2002. Sedimentation in a volcanically dammed valley, Brúarjökull, northeast Iceland. Quaternary Science Reviews 21, 1677–1692.
Koppes, M.N., Hallet, B., 2002. Influence of rapid glacial retreat on the rate of erosion by tidewater glaciers. Geology 30, 47–50.
Koppes, M.N., Hallet, B., 2006. Erosion rates during rapid deglaciation in Icy Bay, Alaska. Journal of Geophysical Research 111, F02023.
Koppes, M., Montgomery, D.R., 2009. The relative efficacy of fluvial and glacial erosion over modern to orogenic timescales. Nature Geoscience 2, 644–647.
Korup, O., Schlunegger, F., 2007. Bedrock landsliding, river incision, and transience of geomorphic hillslope-channel coupling: evidence from inner gorges in the Swiss Alps. Journal of Geophysical Research 112, F03027.
Kühni, A., Pfiffner, O.A., 2001. The relief of the Swiss Alps and adjacent areas and its relation to lithology and structure: topographic analysis from a 250-m DEM. Geomorphology 41, 285–307.
MacGregor, K.C., Anderson, R.S., Anderson, S.P., Waddington, E.D., 2000. Numerical simulations of glacial valley longitudinal profile evolution. Geology 28, 1031–1034.
Mägert, M., 1998. Sedimentation und Entwicklung des Beichlen-Schuttfächers (Untere Süsswassermolasse-Entlebuch). MSc Thesis, University of Bern, Switzerland, p. 176.
Matter, A., 1964. Sedimentologische Untersuchungen im östlichen Napfgebiet (Entlebuch — Tal der Grossen Fontanne, Kt. Luzern). Eclogae Geologicae Helvetiae 57, 315–428.
Mitchell, W.A., Taylor, P.J., Osmaston, H., 1999. Quaternary geology in Zanskar, NW Indian Himalaya: evidence for restricted glaciation and proglacial topography. Journal of Asian Earth Sciences 17, 307–318.
Mollet, H., 1921. Geologie der Schafmatt-Schimberg-Kette und ihrer Umgebung (Kt. Luzern). Beiträge zur Geologischen Karte der Schweiz NF 21, Switzerland, p. 121.
Montgomery, D.R., Buffington, J.M., 1997. Channel reach morphology in mountain drainage basins. Geological Society of America Bulletin 109, 596–611.
Montgomery, D.R., Korup, O., 2011. Preservation of inner gorges through repeated Alpine glaciations. Nature Geoscience 4, 62–67.
Müller, B.U., Schlüchter, C., 1997. Zur Stellung der Zeller Schotter in der alpinen Eiszeiten-Chronologie und ihre stratigrafische Beziehung zu den Schieferkohlen von Gondiswil. Eclogae Geologicae Helvetiae 90, 211–227.
Ng, F.S.L., Barr, I.D., Clark, C.D., 2010. Using the surface profiles of modern ice masses to inform palaeo-glacier reconstruction. Quaternary Science Reviews 29, 3240–3255.
Nye, J.F., 1952. The mechanics of glacier flow. Journal of Glaciology 2, 82–93.
Ouimet, W.B., Whipple, K.X., Crosby, B.T., Johnson, J.P., Schildgen, T.F., 2008. Epigenetic gorges in fluvial landscapes. Earth Surface Processes and Landforms 33, 1993–2009.
Pfiffner, O.A., Erard, P.F., Stäuble, M., 1997. Two cross sections through the Swiss Molasse basin. In: Pfiffner, O.A., Lehner, P., Heitzmann, P., Müller, S., Steck, A. (Eds.), Deep Structure of the Swiss Alps: Results from the National Research Program 20 (NRP 20). Schweizerische Geologische Kommission, Birkhäuser, Basel, Switzerland, pp. 64–72.
Preusser, F., Reitner, J.M., Schlüchter, C., 2010. Distribution, geometry, age and origin of overdeepened valleys and basins in the Alps and their foreland. Swiss Journal of Geosciences 103, 407–426.

Rudoy, A.N., 2002. Glacier-dammed lakes and geological work of glacial superfloods in the Late Pleistocene, Southern Siberia, Altai Mountains. Quaternary International 87, 119–140.
Schlunegger, F., Schneider, H., 2005. Relief-rejuvenation and topographic length scales in a fluvial drainage basin, Napf area, central Switzerland. Geomorphology 69, 102–117.
Schlunegger, F., Burbank, D.W., Matter, A., Engesser, B., Mödden, C., 1996. Magnetostratigraphic calibration of the Oligocene to Middle Miocene (30–15 Ma) mammal biozones and depositional sequences of the Swiss Molasse basin. Eclogae Geologicae Helvetiae 89, 753–788.
Sharpe, D.R., Shaw, J., 1989. Erosion of bedrock by subglacial meltwater, Cantley, Quebec. Geological Society of America Bulletin 101, 1011–1020.
Shreve, R.L., 1972. Movement of water in glaciers. Journal of Glaciology 11, 205–214.
Sjogren, D.B., Fisher, T.G., Taylor, L.D., Jol, H.M., Munro-Stasiuk, M.J., 2002. Insipient tunnel channels. Quaternary International 90, 41–56.
Stock, J.D., Montgomery, D.R., Collins, B.D., Dietrich, W.E., Sklar, L.S., 2005. Field measurements of incision rates following bedrock exposure: implications for process controls on the long profiles of valleys cut by rivers and debris flows. Geological Society of America Bulletin 117, 174–194.
Sugden, D.W., Denton, G.H., Marchant, D., 1991. Subglacial meltwater channel systems and ice sheet overriding, Asgard Range, Antarctica. Geografiska Annaler 73A, 109–121.
Valla, P.G., van der Beek, P.A., Carcaillet, J., 2009. Dating bedrock gorge incision in the French Western Alps (Ecrins-Pelvoux massif) using cosmogenic ^{10}Be. Terra Nova 22, 18–25.
Whipple, K.X., 2004. Bedrock rivers and the geomorphology of active orogens. Annual Review of Earth and Planetary Sciences 32, 151–185.